JB
Journals.ASM.org

Cyclic Di-GMP Riboswitch-Regulated Type IV Pili Contribute to Aggregation of *Clostridium difficile*

Eric Bordeleau,[a] Erin B. Purcell,[b] Daniel A. Lafontaine,[a] Louis-Charles Fortier,[c] Rita Tamayo,[b] Vincent Burrus[a]

Département de Biologie, Faculté des Sciences, Université de Sherbrooke, QC, Canada[a]; Department of Microbiology and Immunology, University of North Carolina, Chapel Hill, North Carolina, USA[b]; Département de Microbiologie et d'Infectiologie, Faculté de Médecine et Sciences de la Santé, Université de Sherbrooke, QC, Canada[c]

Clostridium difficile **is an anaerobic Gram-positive bacterium that causes intestinal infections with symptoms ranging from mild diarrhea to fulminant colitis. Cyclic diguanosine monophosphate (c-di-GMP) is a bacterial second messenger that typically regulates the switch from motile, free-living to sessile and multicellular behaviors in Gram-negative bacteria. Increased intracellular c-di-GMP concentration in *C. difficile* was recently shown to reduce flagellar motility and to increase cell aggregation. In this work, we investigated the role of the primary type IV pilus (T4P) locus in c-di-GMP-dependent cell aggregation. Inactivation of two T4P genes, *pilA1* (CD3513) and *pilB1* (CD3512), abolished pilus formation and significantly reduced cell aggregation under high c-di-GMP conditions. *pilA1* is preceded by a putative c-di-GMP riboswitch, predicted to be transcriptionally active upon c-di-GMP binding. Consistent with our prediction, high intracellular c-di-GMP concentration increased transcript levels of T4P genes. In addition, single-round *in vitro* transcription assays confirmed that transcription downstream of the predicted transcription terminator was dose dependent and specific to c-di-GMP binding to the riboswitch aptamer. These results support a model in which T4P gene transcription is upregulated by c-di-GMP as a result of its binding to an upstream transcriptionally activating riboswitch, promoting cell aggregation in *C. difficile*.**

The Gram-positive spore-forming bacterium *Clostridium difficile* is the leading cause of nosocomial diarrhea and antibiotic-associated colitis in hospital settings (1). Illness caused by *C. difficile* infections (CDI) may range from mild diarrhea to life-threatening, fulminant colitis. Throughout its life cycle, *C. difficile* has to cope with multiple changing environments. In the early steps of CDI, in order to colonize the colon and produce toxins, *C. difficile* spores first germinate in the intestine in response to stimuli such as the presence of bile salts (2, 3). Vegetative cells need to reach the colon, likely attaching to and colonizing the gut mucosa, where they proliferate and produce toxins. Hence, *C. difficile* arguably needs to sense and integrate multiple environmental stimuli in order to coordinate the expression of its colonization and virulence factors during its journey through the gastrointestinal tract. The mechanisms allowing this adaptability in *C. difficile* have been the focus of many recent studies, including those on the *agr* quorum-sensing system, alternative sigma factors, two-component systems, the global transcription regulator CodY, and the sigma factor TcdR, which promotes TcdA and TcdB toxin expression (4–9).

One way by which bacteria sense and respond to changes in their environment is through signal transduction involving secondary messenger molecules. The bacterial second messenger 3′-5′ cyclic diguanosine monophosphate (c-di-GMP) plays multiple key roles in bacterial physiology and virulence (10–12). c-di-GMP has been shown to antagonistically control the motility of planktonic cells and biofilm formation in several bacterial species. An increase in the intracellular c-di-GMP concentration typically induces exopolysaccharide synthesis and adhesion while inhibiting flagellar motility, thereby favoring biofilm formation. A low concentration of the second messenger has an opposite effect. c-di-GMP also controls cell differentiation in *Caulobacter crescentus* (13) and virulence of important human pathogens, including *Vibrio cholerae* (14), *Borrelia burgdorferi* (15), and *Pseudomonas aeruginosa* (16). c-di-GMP turnover is controlled by two groups of enzymes with antagonistic activities. The diguanylate cyclases (DGCs) contain a GGDEF domain and synthesize c-di-GMP from two GTP molecules, whereas the c-di-GMP phosphodiesterases (PDEs) contain an EAL domain or an HD-GYP domain and hydrolyze c-di-GMP into linear pGpG or two GMP molecules, respectively (17–21). Several c-di-GMP effectors are responsible for the regulatory function of c-di-GMP through transcriptional, posttranscriptional, translational, and protein-protein interaction mechanisms. A major class of c-di-GMP effector proteins and the first ever described are the PilZ domain c-di-GMP-binding proteins (22). Although PilZ effectors are numerous, there are also other c-di-GMP-binding effectors, such as the unrelated transcription factors FleQ in *P. aeruginosa* and VpsT in *V. cholerae* (23, 24). In addition to protein effectors, c-di-GMP is also sensed by RNA effectors, the type I and type II c-di-GMP riboswitches (25, 26). Riboswitches are structured RNA regions typically located in the 5′ untranslated regions of diverse bacterial mRNAs. Riboswitches are composed of two modular regions: an aptamer that recognizes and binds a specific metabolite and an expression platform that in most cases controls the expression of the downstream gene(s) (for recent reviews, see references 27 and 28). Ligand

Received 22 September 2014 **Accepted** 9 December 2014

Accepted manuscript posted online 15 December 2014

Citation Bordeleau E, Purcell EB, Lafontaine DA, Fortier L-C, Tamayo R, Burrus V. 2015. Cyclic di-GMP riboswitch-regulated type IV pili contribute to aggregation of *Clostridium difficile*. J Bacteriol 197:819–832. doi:10.1128/JB.02340-14.

Editor: J. S. Parkinson

Address correspondence to Vincent Burrus, Vincent.Burrus@USherbrooke.ca.

Supplemental material for this article may be found at http://dx.doi.org/10.1128/JB.02340-14.

doi:10.1128/JB.02340-14

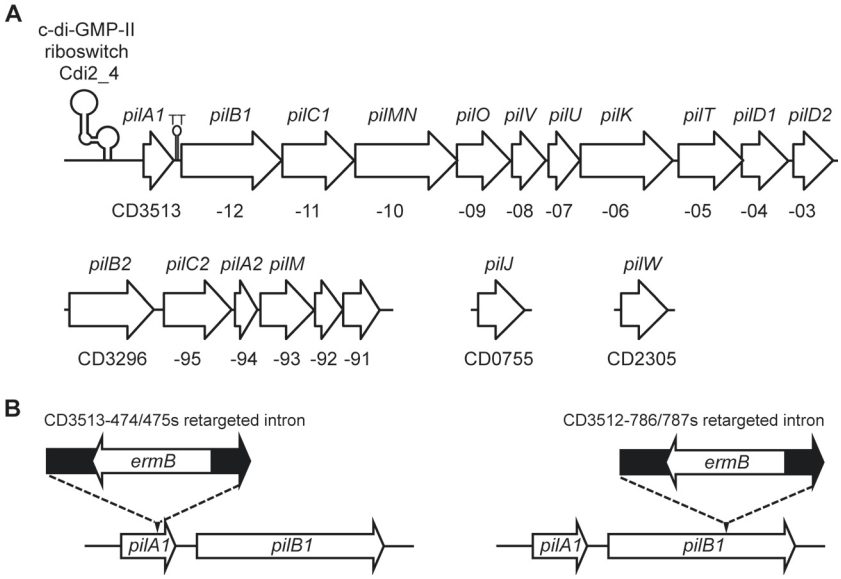

FIG 1 Schematic representation T4P genes. (A) Genes of the primary T4P locus (CD3513 to CD3503) are downstream of a predicted c-di-GMP-II riboswitch (Cdi2_4). ORF numbers (bottom) have been abbreviated for clarity and gene annotations (top) are indicated, as proposed by Maldarelli et al. (42) (see Table S1 in the supplemental material). A transcriptional terminator (TT) is predicted 36 bp downstream of *pilA1* (see Fig. S6A). (B) The *pilA1* and *pilB1* mutant strains were generated using the ClosTron system, and introns were retargeted to insert in the sense orientation in *pilA1* between nucleotides 474 and 475 (CD3513-474/475s intron) or in *pilB1* between nucleotides 786 and 787 (CD3512-786/787s intron).

binding typically leads to repression of gene expression, most commonly through transcription termination or inhibition of translation initiation.

The genome of *C. difficile* 630 codes for 18 predicted DGCs and 19 predicted PDEs, many of which have confirmed enzymatic activity (29, 30). Sudarsan et al. (26) revealed the presence of a c-di-GMP-I riboswitch, Cd1, upstream of the *flgB* gene, which is part of one of two loci encoding the flagellum genes in *C. difficile*. *In vitro* studies have shown that binding of c-di-GMP to Cd1 promotes premature termination of transcription, suggesting that the expression of flagella in *C. difficile* would be repressed by c-di-GMP (26). Purcell et al. (31) demonstrated that overexpression of the DGC DccA (CD1420) in *C. difficile* increases the intracellular c-di-GMP level, which was also associated with a decreased transcription of flagellum genes and reduced bacterial motility. In addition to decreasing motility, DccA overexpression seemed to promote aggregation of *C. difficile* cells by an unknown mechanism (31). The antagonistic regulation by c-di-GMP of motility and sessile behaviors, namely, aggregation and biofilm formation, was also recently reported by Souturina et al. (32). The zinc metalloprotease Zmp1 encoded by CD2830, which is located downstream of the c-di-GMP-I riboswitch Cdi1_12, was recently found to cleave fibronectin, fibrinogen (33), the putative adhesin CD2831, and the putative surface protein CD3246, the last two encoded by genes located downstream of the c-di-GMP-II riboswitches Cdi2_3 and Cdi2_1, respectively (34).

One of the four predicted c-di-GMP-II riboswitches in *C. difficile* 630, Cdi2_4, is located less than 200 bp upstream of a predicted locus for type IV pili (T4P) (25) (Fig. 1A). T4P are surface appendages involved in many phenotypes in Gram-negative bacteria such as *P. aeruginosa* and *Neisseria* spp., including but not limited to adhesion, surface motility (twitching and gliding), biofilm formation and development, cell aggregation, DNA uptake, and phage absorption (for reviews, see references 35 and 36). T4P are thin fibers (6 to 9 nm) that can extend several micrometers in length (37). These fibers are made by the T4P secretion machinery, a type II-related secretion system that promotes pilus elongation by addition of pilin subunits, and may also retract pili by depolymerization of pilin subunits, both at the proximal end of the pilus. T4P gene loci have been predicted for many other Gram-positive bacteria, including several *Clostridium* species (38–40). *C. difficile* T4P genes are mainly located in one primary cluster of genes extending from CD3513 to CD3503 that is predicted to code for all proteins sufficient for T4P formation (Fig. 1A; see also Table S1 in the supplemental material) (41, 42). Herein, we demonstrate a role for T4P in cell aggregation of *C. difficile* and the regulation of T4P expression through binding of the second messenger c-di-GMP to Cdi2_4, a transcriptional riboswitch upstream of the primary T4P locus.

MATERIALS AND METHODS

Bacterial strains and growth conditions. The bacterial strains and plasmids used in this study are described in Table 1. *C. difficile* strains were grown in brain heart infusion (BHI) medium (BD; Bacto) or in BHI medium supplemented with yeast extract (5 g/liter) and 0.1% L-cysteine-HCl (BHIS) (43) at 37°C in an atmosphere of 90% N_2, 10% CO_2, and 5% H_2 in an anaerobic chamber (Coy Laboratory Products). Media for growth of *C. difficile* were supplemented with 10 μg/ml of thiamphenicol (BHIS-tm) and 100 μg/ml of kanamycin (BHIS-tm-km), 10 μg/ml of norfloxacin, and/or 2.5 μg/ml of erythromycin, as appropriate. *Escherichia coli* strains were routinely grown at 37°C under aerobic conditions in Luria-Bertani (LB) medium supplemented with 25 μg/ml of chloramphenicol or 100 μg/ml of ampicillin as needed. For induction of gene expression in the strains carrying vectors with genes under the control of the cationic antimicrobial peptide inducible *cpr* promoter (P_{cpr}), BHIS-tm was supplemented with 1 μg/ml of nisin (2.5%, wt/wt; MP Biomedicals).

TABLE 1 Bacterial strains and plasmids used in this study

Strain or plasmid	Description	Reference or source
Strain name or genotype		
Clostridium difficile		
630	Epidemic type X	38
630 Δ*erm*	Erythromycin-sensitive mutant of *C. difficile* 630	87
pilA1	630 Δ*erm* CD3513-474s::CT	This study
pilB1	630 Δ*erm* CD3512-786s::CT	This study
sigD	630 Δ*erm* CD0266-228s::TT	This study
E. coli CA434	HB101 carrying plasmid R702	88
Plasmids		
pCR2.1-TA	TA cloning vector	Life Technologies
pCR2.1-Rb3513sr	pCR2.1-TA with transcription template for Cdi2_4 c-di-GMP-II riboswitch	This study
pCR2.1-Rb3513sr-a70c	pCR2.1-Rb3513 with A-to-C substitution at nucleotide 70	This study
pCR2.1-Rb3513sr-a70g	pCR2.1 with with A-to-G substitution at nucleotide 70	This study
pMTL007C-E5-CD3513-474/475s	pMTL007C-E5 with the Ll.ltrB intron retargeted to insert after base 474 in the 630 Δ*erm* CD3513 ORF	This study
pMTL007C-E5-CD3512-786/787s	pMTL007C-E5 with the Ll.ltrB intron retargeted to insert after base 786 in the 630 Δ*erm* CD3512 ORF	This study
pBL64	pCR2.1-intron template part A	48
pBL65	pCR2.1-intron template part B	48
pBL100::*sigD*::*ermB*	pBL100 with the group II intron-TargeTron (TT) retargeted to insert after base 228 in the 630 Δ*erm* CD0266 ORF	This study
pMC-Pcpr	*cprK* promoter cloned into pMC123 *E. coli- C. difficile* shuttle vector; *bla catP*	31
pDccA	pMC-Pcpr with DccA downstream of *Pcpr*	31
pDccA^{mut}	pMC-Pcpr with DccA(AADEF) downstream of *Pcpr*	31
pDccA-*RB-pilA1*	pDccA with CD3513 and 497 bp upstream including the Cdi2_4 riboswitch	This study
pDccA^{mut} -*RB-pilA1*	pDccA^{mut} with CD3513 and 497 bp upstream including the c-di-GMP riboswitch	This study
pDccA-*RB*^{A70C}-*pilA1*	pDccA-*RB-pilA1* with - to-C substitution at nucleotide 70 in Cdi2_4	This study
pDccA-*RB*^{A70G}-*pilA1*	pDccA-*RB-pilA1* with A-to-G substitution at nucleotide 70 in Cdi2_4	This study
pDccA-*RB-pilA1*^{G9Y}	pDccA-*RB-pilA1* with G- to-Y substitution at amino acid 9 in PilA1	This study

Plasmid and strain construction. The *pilA1* and *pilB1* genes were insertionally inactivated using a group II intron retargeting approach (44) adapted for *Clostridium*, the ClosTron, as previously described (45). Briefly, the Ll.ltrB intron derivative in plasmid pMTL007C-E5 was retargeted to insert after position 474 of CD3513 (pMTL007C-E5-CD3513-474/475s) or after position 786 of CD3512 (pMTL007C-E5-CD3512-786/787s) using the Perutka algorithm (46) implemented at http://clostron.com to predict suitable intron insertion sites and determine the corresponding intron sequence modifications required. Both pMTL007C-E5 derivatives were synthesized by DNA2.0 (Menlo Park, CA). *E. coli* CA434 was transformed by electroporation and used as a donor strain to transfer plasmids by conjugation into a *C. difficile* 630 Δ*erm* strain. Transconjugants were plated on BHIS agar plates with thiamphenicol to select for the plasmid and norfloxacin to select against *E. coli*. Integrants could be isolated by subsequently culturing transconjugants on BHIS agar plates supplemented with erythromycin. Loss of the plasmid after overnight growth in BHIS broth was then confirmed by sensitivity to thiamphenicol. Intron insertion and orientation in *pilA1* or *pilB1* was confirmed by PCR screening using primer pairs CD3513-282s-F/LCF439 or CD3512-795s-F/LCF439 (see Table S2 in the supplemental material). Insertion of only one intron copy was confirmed by Southern blotting hybridization (see Fig. S1 in the supplemental material).

The *sigD* mutant was generated using a group II intron retargeting approach with a modified set of template and delivery plasmids (45, 47, 48). The intron was retargeted to insert within *sigD* (*fliA*, CD0266) after position 228, an insertion site previously used to inactivate this gene (5). The retargeted intron fragment was generated by PCR, amplifying one portion from pBL64 using primer pair EBSuniv/sigDibs1 and the other portion from pBL65 using primer pair sigDebs1/sigDebs2. The reaction products were mixed and used as the template in a PCR with primer pair sigDibs1/sigDebs1, splicing the two initial PCR products together. The intron fragment was digested with BsrGI and HindIII and cloned into pBL100. The resulting plasmid, pBL100::*sigD*::*ermB*, was then introduced into *E. coli* HB101(pRK24) by electroporation. The pBL100::*sigD*::*ermB* plasmid was conjugated into the *C. difficile* 630 Δ*erm* strain, and transconjugants were selected on BHIS-tm-km. Isolates with intron insertions were selected by screening transconjugants for resistance to erythromycin and then verified to have an insertion in *sigD* by PCR with primer pair sigDqF/EBSuniv. The mutant was further confirmed to be nonmotile using a soft-agar assay (31).

For complementation studies, *pilA1* and the upstream 497-bp region encompassing the c-di-GMP-II riboswitch Cdi2_4 and putative promoter region were amplified by PCR using primer pair RB3513-F2-EcoRI/CD3513-R3-EcoRI, digested with EcoRI, and ligated into the EcoRI-digested pDccA and pDccA^{mut} plasmids. The resulting pDccA-*RB-pilA1* and pDccA^{mut}-*RB-pilA1* plasmids were verified by DNA sequencing. In both plasmids, the P_{cpr} promoter and the promoter of *pilA1* are divergent (see Fig. S2 in the supplemental material). Plasmid pDccA-*RB-pilA1*^{G9Y}, which codes for the PilA1 pilin mutant with a glycine-to-tyrosine amino acid substitution at position 9, and plasmids pDccA-*RB*^{A70C}-*pil1A* and pDccA-*RB*^{A70G}-*pilA1*, which contain adenine-to-cytosine and adenine-to-guanine substitutions at position 70 of Cdi2_4, respectively, were generated by site-directed mutagenesis of pDccA-*RB-pilA1* using the QuikChange Lightning site-directed mutagenesis kit (Agilent Technologies) and primer pairs listed in Table S2 in the supplemental material. Mutated plasmids were verified by DNA sequencing.

For *in vitro* transcription assays, a synthetic transcription template containing the *Bacillus subtilis glyQS* promoter sequence, a GC dinucle-

otide transcription start site, and the Cdi2_4 riboswitch sequence, including 17 bp upstream of the predicted P1 stem and 93 bp downstream of the last base of the predicted transcription attenuator stem, was generated in three steps. First, the 135-bp *glyQS* promoter sequence, followed by a GC sequence, was generated by polymerase cycling assembly (PCA) using oligonucleotides GlyQS-F1 (0.5 μM), GlyQS-R1 (40 pM), GlyQS-F2 (40 pM), and GlyQS-R2 (0.5 μM) as previously described (49). The 229-bp extended Cdi2_4 sequence was amplified by PCR using primers GlyQS-RB3513-F2 and GlyQS-RB3513-R. The final template sequence was then generated by PCR amplification with primers GlyQS-RB3513-F and GlyQS-RB3513-R using the purified and 1:1,000-diluted PCA and PCR products as templates and cloned in pCR2.1-TA (Life Technologies) to generate plasmid pCR2.1-Rb3513sr. Plasmids pCR2.1-Rb3513sr-a70c and pCR2.1-Rb3513sr-a70g, which contain, respectively, adenine-to-cytosine and adenine-to-guanine substitutions at position 70 of the c-di-GMP-II riboswitch, were generated by site-directed mutagenesis of pCR2.1-Rb3513sr using the QuikChange Lightning site-directed mutagenesis kit and primer pairs listed in Table S2 in the supplemental material.

Transmission electron microscopy. Bacteria were inoculated 1:50 from saturated overnight cultures into filter-sterilized BHIS-tm with 1 μg/ml of nisin and grown anaerobically at 37°C for 12 h. Bacteria from 4 ml of culture were centrifuged for 2 min, resuspended in 1 ml of phosphate-buffered saline (PBS) and 4% paraformaldehyde, and fixed in the anaerobic chamber for 45 min. A total of 2.5 μl of cell suspension was adsorbed onto Formar/carbon copper grids (Ted Pella, Inc., Redding CA) for 2 min, washed twice in filtered deionized water, and stained for 30 s in two sequential drops of 1% aqueous uranyl acetate. Cells were observed on a LEO EM 910 transmission electron microscope (Carl Zeiss Microscopy, LLC, Thornwood, NY) and recorded with a Gatan Orius SC1000 digital camera with Digital Micrograph 3.11.0 software (Gatan, Inc., Pleasanton, CA). All of the cells in 15 (wild type [WT]), 20 (*pilA1* and *pilB1*) or 50 (*sigD*) randomly selected grid squares were photographed at a magnification of ×8,000. The images were blinded for quantification as follows: the numbers of cells and pili in each image were recorded by three observers who were unaware of the experimental conditions.

Aggregation assays. Cell aggregation in liquid cultures was monitored as previously reported (31). Briefly, borosilicate tubes containing 10 ml of BHIS-tm with or without nisin were inoculated with colonies from 24- to 48-h-old BHIS-tm plates and incubated 16 h at 37°C. Aggregation was assessed by measuring the cell density (optical density at 600 nm [OD_{600}]) on the culture tubes before (OD_{pre}) and after (OD_{post}) vortexing to resuspend the cell aggregates. The percentage of cells at the bottom of culture tubes was inferred using the following formula: $[(OD_{post} - OD_{pre})/OD_{post}] \times 100$. Monitoring of cell aggregation over time was carried out in fresh BHIS-tm broth with or without nisin inoculated 1/50 with 16-h-old cultures in BHIS-tm and incubated at 37°C. Cell density (OD_{600}) was measured on static cultures over a 10-h incubation time, after which the tubes were vortexed to resuspend the aggregates and measure the cell density of the total population in each tube.

Molecular biology methods. All the enzymes used in this study were obtained from New England BioLabs (NEB) and were used according to the manufacturer's instructions. Plasmid DNA from *E. coli* was prepared with an EZ-10 Spin Column Plasmid DNA Minipreps kit (Bio Basic). Genomic DNA for PCR verification of *C. difficile* clones was crudely extracted by boiling cell pellets of overnight cultures in 5% Chelex 100, 200 to 400 mesh (Bio-Rad). Genomic DNA isolation for quantitative PCR (qPCR) and Southern blot hybridization was performed on 10-ml overnight cultures using the Marmur's method with increased lysozyme concentration (15 mg/ml) and incubation time (2 h) (50). PCR assays were performed with the primers described in Table S2 in the supplemental material in 25-μl PCR mixtures with 1 U of Phusion high-fidelity DNA polymerase. PCR conditions were as follows: (i) 30 s at 98°C, (ii) 30 cycles of 10 s at 98°C, 20 s at a suitable annealing temperature, and 15 to 300 s at 72°C, and (iii) 5 min at 72°C. When needed, PCR products were purified using an EZ-10 Spin Column PCR product purification kit. *E. coli* was transformed by electroporation according to the method of Dower and colleagues (51). Transformation was carried out in 0.1-cm electroporation cuvettes using a Bio-Rad GenePulser Xcell apparatus set at 25 μF, 200 Ω, and 1.8 kV.

RNA isolation and qRT-PCR. RNA was isolated from *C. difficile* cultures grown in BHIS-tm to an OD_{600} of 0.7 without or with 0.1 and 1 μg/ml of nisin. Samples were mixed with an equal volume of cold 1:1 ethanol-acetone and stored at −80°C. Total RNA extraction was achieved using an RNeasy minikit (Qiagen) according to the manufacturer's instructions and glass bead lysis. Cells resuspended in 1 ml of RLT buffer (Qiagen) were submitted to 2 cycles of 40 s at 4 m/s on a Fastprep 24 apparatus (MP Bimedicals) with 0.5 g of 0.1-mm glass beads. Purified RNA samples were then subjected to gDNA digestion using Turbo DNase (Ambion) by following the manufacturer's instructions. Quantitative reverse transcription-PCR (qRT-PCR) assays were performed on the RNomics platform of the Laboratoire de Génomique Fonctionnelle de l'Université de Sherbrooke (http://lgfus.ca). RNA integrity was assessed using an Agilent 2100 Bioanalyzer (Agilent Technologies). Reverse transcription was performed on 2.2 μg of total RNA with Transcriptor reverse transcriptase, random hexamers, deoxynucleoside triphosphates (dNTPs; Roche Diagnostics), and 10 U of RNAseOUT (Invitrogen Life Technologies) according to the manufacturer's protocol in a total volume of 20 μl. All forward and reverse primers were individually resuspended to 20 to 100 μM stock solutions in Tris-EDTA buffer (IDT) and diluted as a primer pair to 1 μM in RNase DNase-free water (IDT). qPCRs were performed in 10-μl volumes in 96-well plates on a CFX-96 thermocycler (Bio-Rad) with 5 μl of 2× iTaq universal SYBR green supermix (Bio-Rad), 10 ng (3 μl) of cDNA, and 200 nM (final concentration; 2 μl) primer pair solutions. The following cycling conditions were used: 3 min at 95°C and 50 cycles of 15 s at 95°C, 30 s at 60°C, and 30 s at 72°C. Relative expression levels were calculated using a model taking into account multiple stably expressed reference genes (52) and housekeeping genes *adk*, *rpoA*, and *gyrA* evaluated by geNorm (53). Primer design (see Table S2 in the supplemental material) and validation were evaluated as described elsewhere (54). In every qPCR run, a no-template control was performed for each primer pair and a no-reverse transcriptase control was performed for each cDNA preparation. Experiments were carried out three times on three biological replicates, and results were combined.

Plasmid copy number quantification. Genomic DNA was isolated from *C. difficile* cultures grown in BHIS to mid-exponential phase (OD_{600} of 0.6) or stationary phase (16 h). Gene copy number was measured by qPCR using 10 ng (3 μl) of genomic DNA (gDNA) as described herein for cDNA quantification (see qRT-PCR) using primers listed in Table S2 in the supplemental material. CD3513 (*pilA1*) was targeted to measure its relative gene copy number in the WT strain harboring plasmids pDccA-*RB-pilA1* or devoid of vector. The data were analyzed using the threshold cycle ($\Delta\Delta C_T$) method using CD3512 (*pilB1*) as the chromosomal copy number reference. Experiments were carried out three times on two biological replicates, and results were combined.

Single-round *in vitro* transcription assays. Transcription reactions were conducted as previously described (55), with minor modifications. Briefly, DNA templates for *in vitro* transcription maintained in plasmids pCR-2.1-Rb3513sr, pCR-2.1-Rb3513sr-a70c, and pCR-2.1-Rb3513sr-a70g were amplified by PCR using primers GlyQS-RB3513-F and GlyQS-RB3513-R. The dinucleotide GpC, fused with the 17 nucleotides (nt) upstream of the predicted P1 stem, was used to initiate transcription. Transcription reactions were expected to stop at the predicted transcription terminator for terminated RNA species (approximately 146 nt) or to stop at the end of the template for read-through species (231 nt). Reaction mixtures containing 300 fmol of DNA template in a buffer containing 150 μM GpC, 2.5 μM ATP and CTP, 0.75 μM UTP, 2 μCi of [α-^{32}P]UTP, 50 mM Tris-HCl (pH 8.0 at 23°C), 20 mM $MgCl_2$, 0.1 mM EDTA, 1 mM dithiothreitol (DTT), 10% glycerol, and c-di-GMP or c-di-AMP (Biolog Life Science Institute, Bremen), when needed, were incubated 5 min at

37°C. Transcription was initiated by addition of 0.25 U of *E. coli* RNA polymerase holoenzyme (Epicentre) and incubation for 15 min at 37°C. Reactions were completed by the addition of each NTP to a final concentration of 2.5 μM and 0.45 mg/ml of heparin to avoid transcription reinitiation. After an additional 15-min incubation period at 37°C, reactions were stopped by addition of an equal volume of 95% formamide. Reaction products were separated on 8% denaturing polyacrylamide gels. Exposed phosphor imager screens were scanned and analyzed using an FX molecular imager and Quantity One software (Bio-Rad). The c-di-GMP concentration needed to obtain half of the change, T_{50}, was determined as described previously (55). Briefly, the T_{50} was analyzed by nonlinear regression curve fitting using GraphPad Prism and the equation $\alpha = RT_i + RT_{max}$ ([c-di-GMP]/(T_{50} + [c-di-GMP]) where α is the percentage of read-through and RT_i and RT_{max} are the initial and maximal changes, respectively, in transcription termination.

RNA molecular markers. In order to verify the length of transcription reaction products, two RNA molecular markers corresponding to the length of the predicted terminated (146 nt) and read-through (231 nt) RNA species were generated using T7 RNA polymerase (Life Technologies). Templates for T7 RNA transcription were prepared by PCR amplification on *C. difficile* 630 genomic DNA using primer pairs T7RB3513-F/GlyQS-RB3513term-R2 and T7RB3513-F/GlyQS-RB3513-R and then purified by denaturing PAGE and electroelution. Both transcripts start with a 5′ GCG sequence to minimize 5′-end heterogeneity of the RNA population (56). RNA labeled at the 5′ end with ^{32}P was obtained by dephosphorylation with shrimp alkaline phosphatase (Affymetrix) and phosphorylation with T4 polynucleotide kinase (NEB) and [γ-^{32}P]ATP according to the manufacturer's instructions. Reactions products were separated by denaturing PAGE, electroeluted, ethanol precipitated, and dissolved in water.

RESULTS

T4P biogenesis is induced by c-di-GMP. Since the putative T4P primary locus in *C. difficile* (open reading frames [ORFs] CD3513 to CD3503) is located downstream of a predicted c-di-GMP-II riboswitch (Fig. 1A), we speculated that T4P are involved in the previously reported aggregation of *C. difficile* cells in liquid culture upon elevation of intracellular c-di-GMP levels (31). CD3513 is the first gene of the T4P primary locus and likely codes for a major pilin subunit (41, 42). Therefore, it is named *pilA1* as proposed by Maldarelli et al. (42). The second gene of the T4P primary locus, CD3512, encodes a homolog of PilB, a predicted hexameric ATPase thought to supply the energy required for pilus assembly through the successive addition of pilin subunits. PilB is essential for T4P secretion in *P. aeruginosa* and *Neisseria gonorrhoeae* (named PilF in *N. gonorrhoeae*) (57, 58). CD3512 and the downstream genes are part of the primary T4P locus and named as proposed by Maldarelli et al. (42); i.e., CD3512 is named *pilB1*, whereas the second *pilB* gene, CD3296, contained in the secondary T4P gene operon (CD3296 to CD3291), is named *pilB2* (Fig. 1A).

Reasoning that the gene located immediately downstream of the c-di-GMP-II riboswitch Cdi2_4 is most likely the gene directly regulated by c-di-GMP, at the transcriptional or translational level, we disrupted the putative pilin gene *pilA1* using the group II intron retargeting approach adapted to clostridia (ClosTron) (Fig. 1B; see also Fig. S2 in the supplemental material). We also disrupted *pilB1* to verify the role of T4P independently of the PilA1 pilin if *pilA1* was not involved in T4P biogenesis (Fig. 1B; see also Fig. S2). The *pilB1* gene could also be regulated by c-di-GMP, as it is located directly downstream of *pilA1*. Although the secondary *pilB2* gene could have a redundant function, we hypothesized that *pilB1* was essential for pilus biogenesis in *C. difficile*. The intracellular c-di-GMP level in the *C. difficile* 630 Δ*erm* strain (WT), or its *pilA1* and *pilB1* mutants, was manipulated by introducing pDccA to express the *C. difficile* DGC DccA under a nisin-inducible promoter as described before (31). The empty vector (pMC-Pcpr) was used as a negative control (Table 1).

Examination of the cells by transmission electron microscopy revealed that upon expression of DccA in the WT strain, c-di-GMP induces the formation of pilus-like structures while inhibiting biosynthesis of flagella (Fig. 2A). In contrast, the WT strain with the empty vector displayed many flagella but no pili at its surface under the same inducing conditions. Interestingly, the average number of pili/cell was only ~2.4, as many cells did not display any pili (Fig. 2B; see also Fig. S3A in the supplemental material). To verify that the appendages observed on the WT strains expressing DccA were not flagella, we also used a *sigD* (*fliA*, σ28) disruption mutant of the *C. difficile* 630 Δ*erm* strain, which exhibits impaired motility (Fig. 2A) (59). The average number of pili/cell for the *sigD* strain expressing DccA was comparable to that for the WT strain expressing DccA (Fig. 2B; see also Fig. S3A). No flagellum or pilus could be detected on the surface of the *sigD* mutant strain carrying the empty vector. Disruption of either *pilA1* or *pilB1* virtually abolished the formation of pilus-like structures at the surface of the cells despite DccA expression sufficient to almost completely abolish flagellum formation. Moreover, mature PilA1 pilin could be detected in extracellular fractions upon DccA expression in the WT strain but not in the *pilA1* or *pilB1* mutant (see Fig. S3B). Collectively, these results support the notion that the observed appendages induced by c-di-GMP are T4P, as they require predicted T4P genes *pilA1* and *pilB1* (and/or the downstream T4P genes) for their biogenesis.

T4P are involved in c-di-GMP-dependent aggregation. To investigate further the roles of *pilA1* and *pilB1* and of pilus-like structures, we monitored cell aggregation in cultures of the *C. difficile* 630 Δ*erm* strain (WT) and the *pilA1* and *pilB1* mutants bearing pDccA or pDccA^{mut} (Table 1), which expresses a catalytically inactive mutant of DccA unable to produce c-di-GMP. Extensive cell aggregation occurred for the WT strain with pDccA upon nisin induction, with approximately 90% of the cells pelleting to the bottom of the culture tube after a 16-h incubation period (Fig. 3A; see also Fig. S4A in the supplemental material). Under the same conditions, less than 2.5% cell aggregation was observed for the WT strain with pDccA^{mut}, and less than 0.05% cell aggregation was observed for the uninduced WT strain with pDccA (Fig. 3A; see also Fig. S4A). Like the WT strain, neither the *pilA1* nor the *pilB1* mutant strain significantly aggregated upon expression of *dccA*^{mut} or without induction. Interestingly, both mutant strains with pDccA exhibited a 2-fold reduction (*pilA1*, $P = 0.005$; *pilB1*, $P = 0.0028$) compared to the WT strain with pDccA, displaying 40 to 45% cell aggregation upon nisin induction. These observations suggest that *pilA1* and *pilB1* contribute significantly to c-di-GMP-regulated cell aggregation, but an additional c-di-GMP-regulated factor(s) is likely involved.

We noticed that the absorbances of cultures of aggregated cells after resuspension were slightly lower than those of uninduced control cultures (see Fig. S4A in the supplemental material), suggesting that the aggregates could have resulted from the accumulation of dead cells. We verified that the aggregated cells were viable and, most importantly, that observation of the optical density reflected the viable cell counts by comparing the CFU/ml in samples collected before and after suspension of the induced and

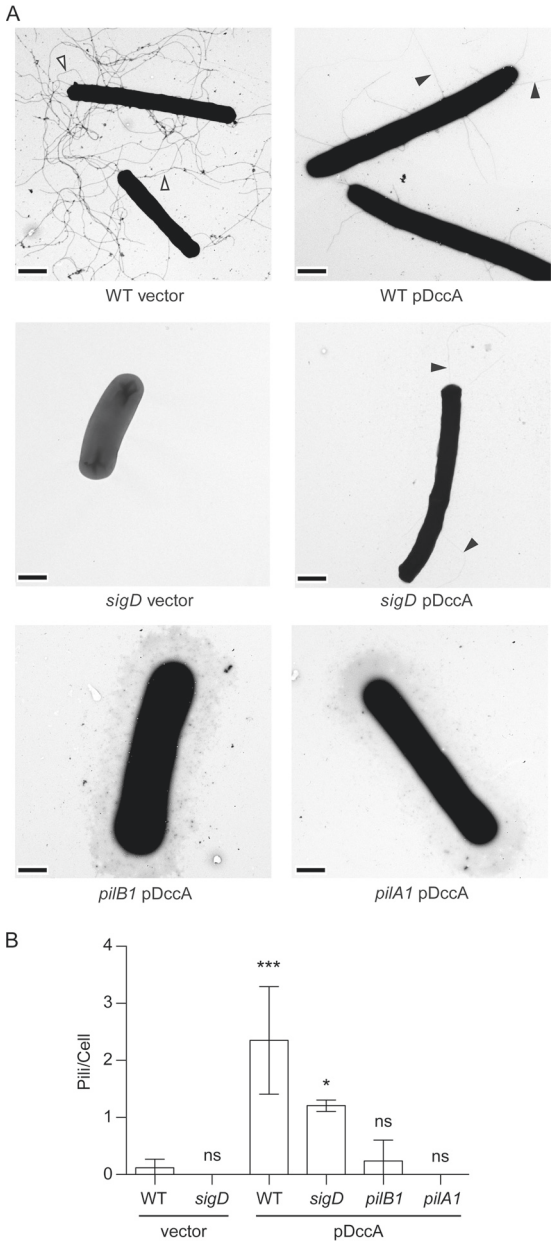

FIG 2 c-di-GMP induces T4P formation. (A) Transmission electron microscopy of the *C. difficile* 630 Δ*erm* strain (WT) or its *sigD* mutant with pDccA or the empty vector and the *pilB1* and *pilA1* mutants with pDccA from 12-h static liquid cultures in BHIS-tm with nisin (1 μg/ml). Scale bars = 1 μm. Open arrowheads show flagella and closed arrowheads show pili. (B) Mean number of pili for each cell in 15 (WT), 20 (*pilA1* and *pilB1*), or 50 (*sigD*) randomly selected grid squares photographed at a magnification of ×8,000. The images were blinded for quantification as described in the text. Data were analyzed by one-way analysis of variance (ANOVA) and Dunnett's multiple-comparison test comparing values to those for the WT strain with the empty vector (ns, $P > 0.05$; ***, $P < 0.001$; *, $P < 0.05$).

uninduced cells carrying pDccA (see Fig. S4C). As expected, culture samples collected before and after resuspension of the aggregates exhibited concentrations of viable cells in agreement with the observed culture absorbance measurements (see Fig. S4A and C). This observation also confirmed that the observed c-di-GMP-dependent aggregation phenotype does not result from cell death and subsequent pelleting of cell debris over time.

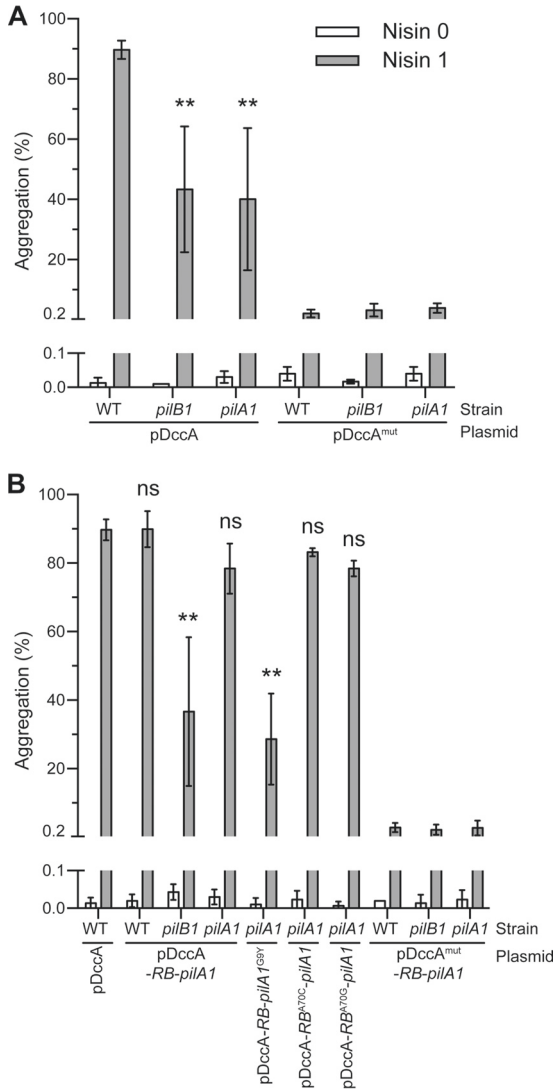

FIG 3 T4P are required for c-di-GMP-dependent aggregation of *C. difficile* planktonic cells. Cell aggregation was monitored by measuring the absorbance (OD_{600}) of supernatants before (OD_{pre}) and after (OD_{post}) vortexing (see Fig. S4A in the supplemental material) for 16-h static liquid cultures in BHIS-tm. Aggregation was expressed as a percentage of cells at the bottom of culture tubes, determined with the equation $[(OD_{post} - OD_{pre})/OD_{post}] \times 100$. (A) Cell aggregation of the *C. difficile* 630 Δ*erm* strain (WT) or its *pilB1* and *pilA1* insertion mutants upon expression of the diguanalyte cyclase DccA (pDccA) or inactive DccA mutant ($pDccA^{mut}$) by induction with 0 or 1 μg/ml of nisin. (B) Cell aggregation complementation assays using the *pilA1* gene and its upstream Cdi2_4 riboswitch cloned into a plasmid expressing DccA (pDccA-*RB-pilA1*) or expressing $DccA^{mut}$ ($pDccA^{mut}$-*RB-pilA1*). Complementation of the *pilA1* mutant was also carried out using plasmids expressing $PilA1^{G9Y}$ (pDccA-*RB-pilA1*^{G9Y}) or containing the nucleotide substitution A70C or A70G in the Cdi2_4 riboswitch (pDccA-RB^{A70C}-*pilA1* and pDccA-RB^{A70G}-*pilA1*). The result for the WT strain with pDccA from panel A was duplicated to ease interpretation. The means and standard deviations obtained from three independent assays are shown. One-way ANOVA with Dunnett's multiple-comparison posttest was used to compare the strains to the WT strain with pDccA (ns, $P > 0.05$; **, $P < 0.01$).

PilA1 pilin complementation restores c-di-GMP-induced aggregation. The lack of cell aggregation in the *pilA1* mutant (as well as in the *pilB1* mutant used in this study as a presumed T4P-negative control) could solely result from polar effects on the ex-

pression of the downstream genes. To rule out this possibility, the wild-type *pilA1* gene and its upstream regulatory region including the c-di-GMP-II riboswitch Cdi2_4 (*RB*) were introduced into pDccA and pDccA^{mut} to generate pDccA-*RB-pilA1* and pDccA^{mut}-*RB-pilA1* for complementation experiments (see Fig. S2 in the supplemental material). Complementation of the *pilA1* mutant using pDccA-*RB-pilA1* increased cell aggregation 2-fold (Fig. 3B), from ~ 40 to 80% compared to the value for the same *pilA1* mutant bearing pDccA (Fig. 3A). Aggregation of the *pilA1* mutant complemented with pDccA-*RB-pilA1* was indistinguishable from that of the WT strain bearing pDccA ($P = 0.88$). Complemented cells also displayed pili at their surface (see Fig. S3A, C, and D).

Complementation of the *pilA1* mutant using a plasmid expressing a PilA1^{G9Y} prepilin leader peptide substitution mutant, pDccA-*RB-pilA1*^{G9Y}, did not restore cell aggregation to WT levels. G9 of PilA1 corresponds to a highly conserved glycine residue located at the −1 position of the predicted cleavage site in the prepilin subunit. This residue was shown to be necessary for the cleavage and subsequent assembly of pilin subunits into pili in *P. aeruginosa* (60). Consistent with this, PilA1^{G9Y} could be detected only in whole-cell lysates and not in the extracellular fraction when the *pilA1* mutant was complemented with pDccA-*RB-pilA1*^{G9Y}, thereby confirming that the G9Y mutation prevents the export of PilA1 and the formation of pili in *C. difficile* (see Fig. S3B in the supplemental material). The *pilA* mutant complemented with *pilA1*^{G9Y} did not display visible pili (see Fig. S3A, C, and D).

As expected, none of the strains containing pDccA^{mut}-*RB-pilA1* (i.e., complemented for *pilA1* but expressing DccA^{mut}) were able to aggregate (Fig. 3B). Finally, the additional copies of the *pilA1* gene in the *pilB1* mutant with pDccA-*RB-pilA1* did not restore cell aggregation to WT levels (Fig. 3B). Altogether, these observations support that the PilA1 pilin itself is involved in c-di-GMP-regulated cell aggregation.

Cell aggregation occurs during exponential growth. c-di-GMP-regulated aggregation was also monitored more closely for all strains by measuring the absorbance of cultures over a 10-h incubation time. Upon nisin induction, cell aggregates of the WT strain with pDccA could be visually observed in suspension after ~5 to 6 h as the cells in suspension reached an OD_{600} of ~0.8 to 0.9 (Fig. 4A). From this breakpoint, longer incubation time resulted in decreased absorbance of the supernatant down to an OD_{600} of ~0.3 after 10 h and in cells accumulating at the bottom of the tube after only 6 h (Fig. 4A and C). Interestingly, cell aggregation was clearly impaired for both the *pilA1* and *pilB1* mutants compared to the WT strain; in the presence of nisin, the absorbance of the culture in suspension continued to increase after 6 h to reach an OD_{600} of ~1.2 to 1.4 after 10 h, although a much reduced cell pellet could also be observed (Fig. 4A and C). In contrast, no cell aggregation could be observed and the absorbance of the cultures increased steadily to reach stationary phase at an OD_{600} of ~2.0 after 10 h for all strains cultured without induction (see Fig. S5A and B in the supplemental material) or strains containing DccA^{mut} induced with nisin (see Fig. S5C).

Interestingly, observation of aggregation over shorter incubation times revealed that while complementation of the *pilA1* mutant using pDccA-*RB-pilA1* seemed to restore the cell aggregation phenotype in overnight cultures (Fig. 3B), it promoted an earlier and more drastic cell aggregation phenotype (Fig. 4). In fact, the absorbance of cells in suspension of both the WT and the *pilA1* mutant strains bearing pDccA-*RB-pilA1* barely increased past the 4-h incubation time, stabilizing to an OD_{600} of ~0.3. Cell aggregates in suspension were already apparent and a pellet became increasingly visible at the bottom of the culture tubes (Fig. 4B and C). Increased cell aggregation is likely caused by the increased *pilA1* copy number provided by pDccA-*RB-pilA1*. Indeed, real-time qPCR experiments confirmed that pDccA-*RB-pilA1* maintains at about 34.2 ± 2.0 and 17.3 ± 0.2 copies per cell in the exponential and stationary phases, respectively. Again, complementation of the *pilA1* mutant by expressing the *pilA1*^{G9Y} mutant from pDccA^{mut}-*RB-pilA1*^{G9Y} (Fig. 4B) did not restore cell aggregation to WT levels and was indistinguishable from the *pilA1* mutant strain containing pDccA (Fig. 4A), thereby confirming that the mature PilA1 pilin is involved in cell aggregation.

c-di-GMP induces the expression of the primary T4P gene cluster. Typically, riboswitches control either mRNA transcription termination through the formation of a Rho-independent terminator stem-loop or translation initiation through the sequestration of the Shine-Dalgarno sequence or start codon. Although PilA1 protein levels were elevated upon increased c-di-GMP levels (see Fig. S3B in the supplemental material), we sought to verify whether it resulted from transcriptional regulation. To assess the effect of increased intracellular c-di-GMP levels on the transcription of the genes downstream of the riboswitch, we carried out real-time quantitative reverse transcription-PCR (qRT-PCR) experiments on cDNAs obtained from total RNAs isolated from the *C. difficile* 630 Δ*erm* strain with either pDccA or pDccA^{mut}. The relative expression of the gene directly downstream of the riboswitch Cd2_4, *pilA1*, increased nearly 40-fold upon high intracellular c-di-GMP levels (Fig. 5A). Likewise, the expression of all genes downstream of *pilA1*, with the exception of *pilD2*, was significantly higher (2- to 10-fold increase) under induced conditions. Expression of the three additional predicted pilin genes *pilJ* (CD0755), *pilW* (CD2305), and *pilA2* (CD3294), located in three distinct chromosomal loci remote from the primary T4P gene cluster, was not significantly modulated by c-di-GMP, as their corresponding transcript levels remained virtually unchanged by increased intracellular levels of c-di-GMP (Fig. 5B). The lower increase in transcript levels for genes downstream of *pilA1* could result from transcription attenuation caused by the presence of a predicted Rho-independent terminator (WebGeSTer DB prediction [61]) located 36 bp downstream of *pilA1* stop codon (Fig. 1A; see also Fig. S6A in the supplemental material). Indeed, *pilA1* and *pilB1* are cotranscribed, as detected by qRT-PCR (see Fig. S7). Furthermore, *pilA1* disruption abolishes the increase of expression of the downstream genes *pilB1* and *pilC1* observed in the WT strain upon high c-di-GMP levels (Fig. 5C). However, c-di-GMP-independent transcription of *pilB1* and downstream genes is also initiated from at least one additional promoter located directly upstream *pilB1* (see Fig. S6B and C).

The T4P primary locus is located downstream of a functional transcriptional c-di-GMP-II riboswitch. Our analysis of T4P gene expression suggested that Cdi2_4 is a positive transcriptional riboswitch. Although the predicted secondary structure of the Cdi2_4 riboswitch contains features of a functional c-di-GMP-II aptamer (i.e., P1, P2, P3, and P4/pseudoknot structures), it was not initially predicted to have a transcriptional terminator as an expression platform (25). However, we were able to predict a possible terminator structure in the vicinity of

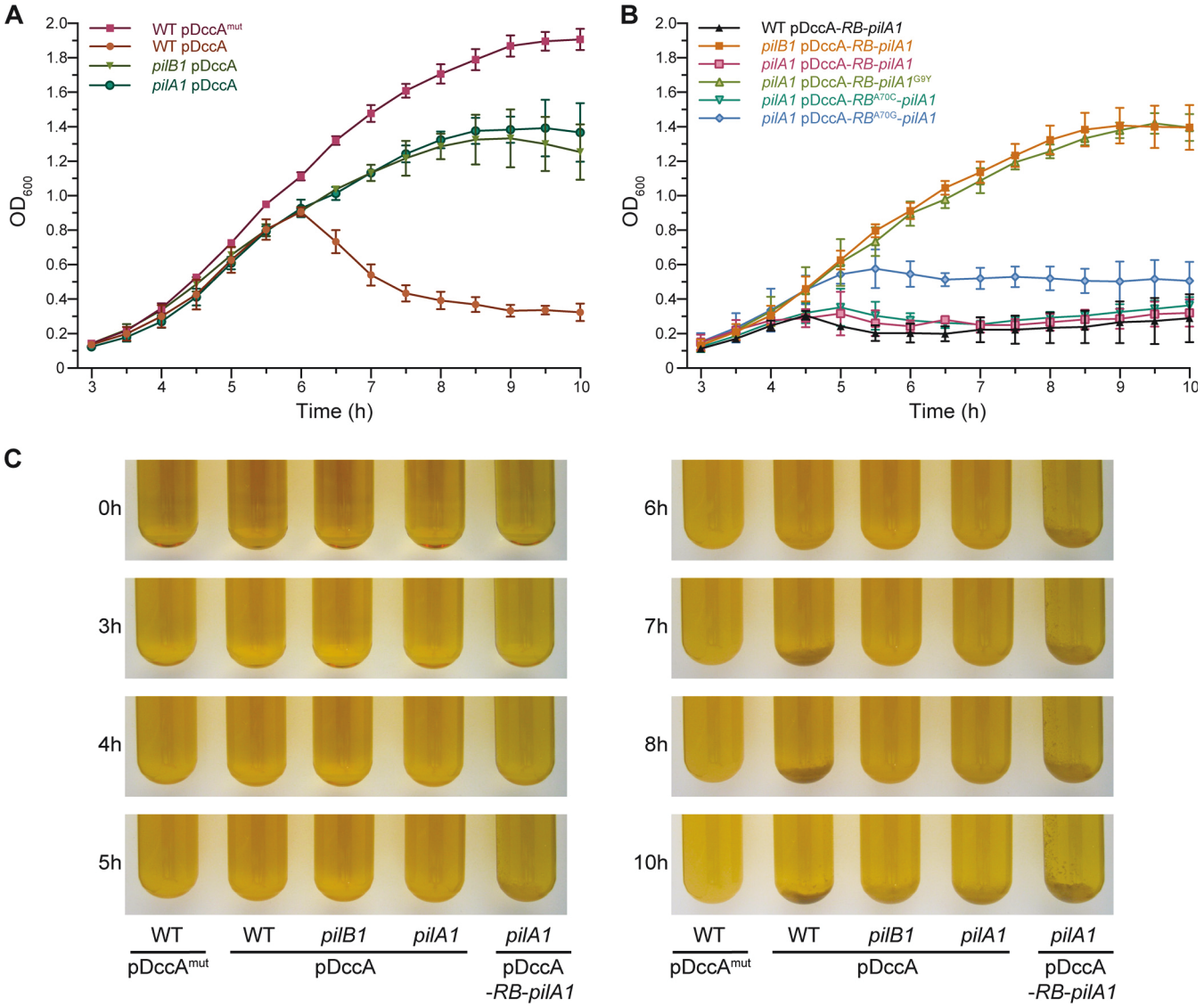

FIG 4 Time course monitoring of cell aggregation reveals differences in aggregation rate. Cell aggregation from static liquid cultures was monitored by measuring the optical densities (600 nm) at 30-min intervals. (A) Cell aggregation of the *C. difficile* 630 Δ*erm* strain (WT) or its *pilB1* and *pilA1* insertion mutants upon expression of the diguanalyte cyclase DccA (pDccA) or inactive DccA mutant (pDccA^{mut}). (B) Cell aggregation complementation assays using plasmids pDccA-*RB-pilA1*, pDccA-*RB-pilA1*^{G9Y}, or pDccA-*RB*^{A70C}*-pilA1* and pDccA-*RB*^{A70G}*-pilA1*. (C) Representative images of the aggregation phenotypes observed in liquid cultures for selected genotypes. The expression of *dccA* or *dccA*^{mut} was induced with 1 μg/ml of nisin. The means and standard deviations obtained from three independent assays are shown. Differences in the duration of the lag phase, independent of the strains, were attenuated by adjusting the time point of the beginning of the exponential phase as in the uninduced control cultures (see Fig. S5 in the supplemental material).

Cdi2_4 using the RNAfold webserver (62). We inferred that formation of the P1 stem upon c-di-GMP binding to the aptamer could act as an antiterminator stem that sequesters the proximal half of a putative Rho-independent terminator stem (Fig. 6A).

To test this hypothesis, a single-round *in vitro* transcription assay was developed to differentiate premature transcription termination from full-length transcription upon c-di-GMP binding. Using this assay, we first demonstrated that c-di-GMP increased transcription past the predicted terminator (Fig. 6B). Indeed, the percentage of read-through transcripts increased with the c-di-GMP concentration (Fig. 6C). Moreover, the amount of c-di-GMP that achieved half of the transcription elongation change, defined as the T_{50} (63), was determined to be 70 ± 12 nM, which is a physiologically relevant concentration in *C. difficile* (31). These results support the notion that binding of c-di-GMP to the Cdi2_4 riboswitch promotes transcription elongation.

The Cdi2_4 aptamer specifically binds c-di-GMP. Smith and colleagues (64) determined the structure and binding pocket nucleotides of a c-di-GMP-II aptamer from *Clostridium acetobutylicum*, Cac-1-2. Modeling of the Cdi2_4 aptamer tertiary structure revealed the conservation of nucleotides involved in ligand recognition through noncanonical base-pairing (A69 and G73) with c-di-GMP guanines and base stacking interactions (A13, A61, and A70) (Fig. 7A) (64). This led us to test

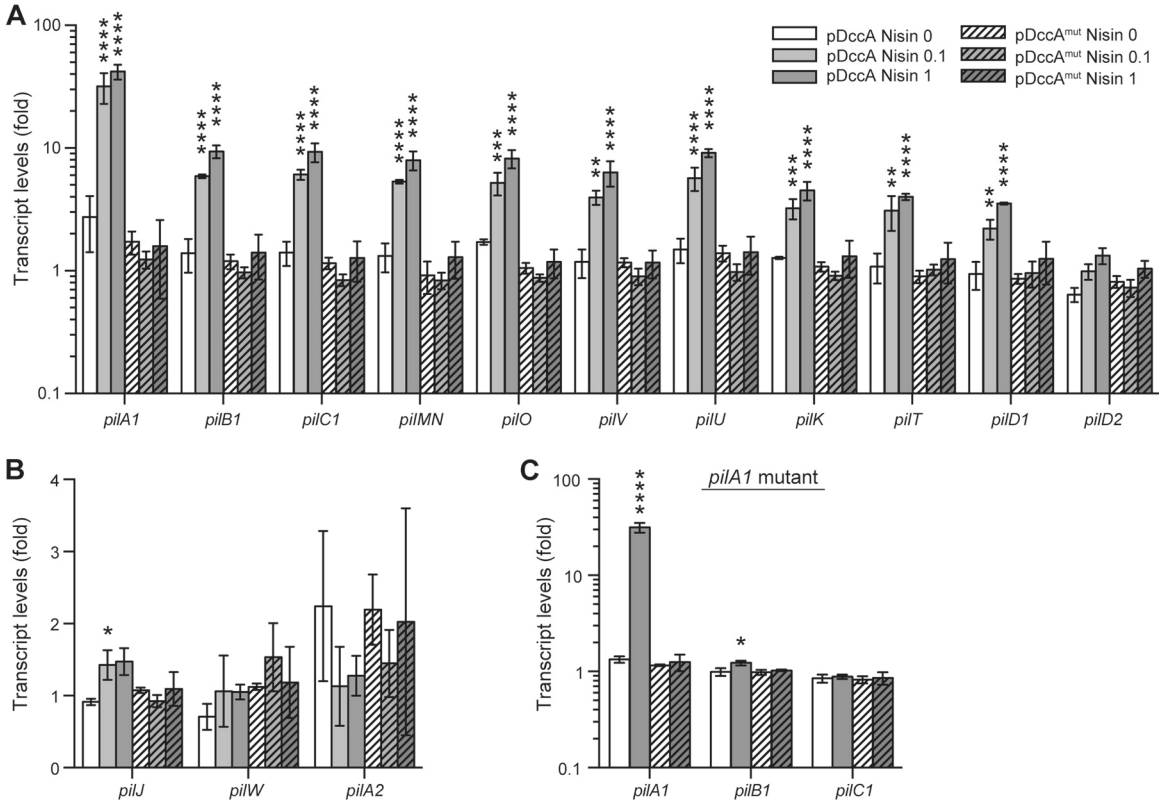

FIG 5 c-di-GMP increases the expression of the T4P primary cluster genes. Shown are relative transcript levels of T4P primary cluster genes (A) and alternative T4P pilin genes (B) in the WT strain and T4P primary cluster genes in the *pilA1* mutant strain background (C). Bars represent the transcript levels (fold) relative to the *C. difficile* 630 Δ*erm* strain containing the pDccA^{mut} control plasmid induced with 1 μg/ml of nisin as determined by qRT-PCR using *adk*, *gyrA*, and *rpoA* as internal references for normalization. The means and standard deviations obtained from three independent assays are shown. One-way ANOVA with Dunnett's multiple-comparison posttest was used to compare the values to that of the strain with the pDccA^{mut} control plasmid induced with 1 μg/ml of nisin (****, $P < 0.0001$; ***, $P < 0.001$; **, $P < 0.01$; *, $P < 0.05$).

whether increased read-through transcription in the presence of c-di-GMP was triggered by its binding to the riboswitch aptamer or by unforeseen interaction of c-di-GMP in single-round transcription assays. Reasoning that mutations in the aptamer that decrease c-di-GMP binding should in return affect the ability of the whole riboswitch to regulate read-through transcription, we generated two single-nucleotide substitutions in Cdi2_4, A70G and A70C, that were shown to reduce the binding affinity of Cac-1-2 25,000- and 2-fold, respectively (64). Similarly, the A70G substitution in Cdi2_4 abolished the effect of c-di-GMP on promoting transcription elongation, while the A70C substitution did not impact considerably the percentage of read-through transcripts (Fig. 7B). To further test the specificity of Cdi2-4 for c-di-GMP, we carried out the same assay using c-di-AMP, a close c-di-GMP analog, and observed that c-di-AMP does not increase the percentage of read-through transcripts. Together, these results support the notion that increased transcription elongation is promoted by specific interactions between c-di-GMP and nucleotides of the Cdi2_4 aptamer binding pocket and support a model in which c-di-GMP promotes T4P genes transcription through binding to the upstream c-di-GMP-II riboswitch.

To assess the importance of the c-di-GMP riboswitch for regulating the expression of *pilA1*, complementation of the *pilA1* mutant by adding plasmids pDccA-*RB*^{A70C}-*pilA1* and pDccA-*RB*^{A70G}-*pilA1* was attempted. As expected, the A70C substitution did not impair Cdi2_4 riboswitch activity, as the *pilA1* mutant with pDccA-*RB*^{A70C}-*pilA1* displayed very similar cell aggregation phenotypes in both overnight cultures and shorter incubation times than the *pilA1* mutant with pDccA-*RB-pilA1* (Fig. 3A and B). Surprisingly, the A70G substitution did not completely prevent complementation of the *pilA1* mutant by plasmid-borne copies of *pilA1* in aggregation assays. Indeed, cell aggregation of the *pilA1* mutant containing pDccA-*RB*^{A70G}-*pilA1* after 16 h of incubation was about 80%, i.e., not significantly lower than that of the WT strain with pDccA or the *pilA1* mutant with pDccA-RB-*pilA1* (Fig. 3B). Closer examination over shorter incubation times also revealed increased cell aggregation of the *pilA1* mutant with pDccA-*RB*^{A70G}-*pilA1* compared to the noncomplemented strain (*pilA1* pDccA), as the optical density of the cells in suspension remained at about 0.5 for the *pilA1* mutant with pDccA-*RB*^{A70G}-*pilA1*, compared to about 1.3 for *pilA1* with *pilA1* pDccA (Fig. 4B). Nevertheless, the A70G substitution seemed to impair the function of the c-di-GMP riboswitch, as cell aggregation of the *pilA1* mutant with pDccA-*RB*^{A70G}-*pilA1* was lower than for the same *pilA1* mutant complemented with pDccA-*RB-pilA1*. After 5 to 6 h of incubation, the absorbance of the cells in suspension of the *pilA1* mutant complemented with pDccA-*RB-pilA1*, or the control riboswitch substitution mutant plasmid pDccA-*RB*^{A70C}-*pilA1*, did not con-

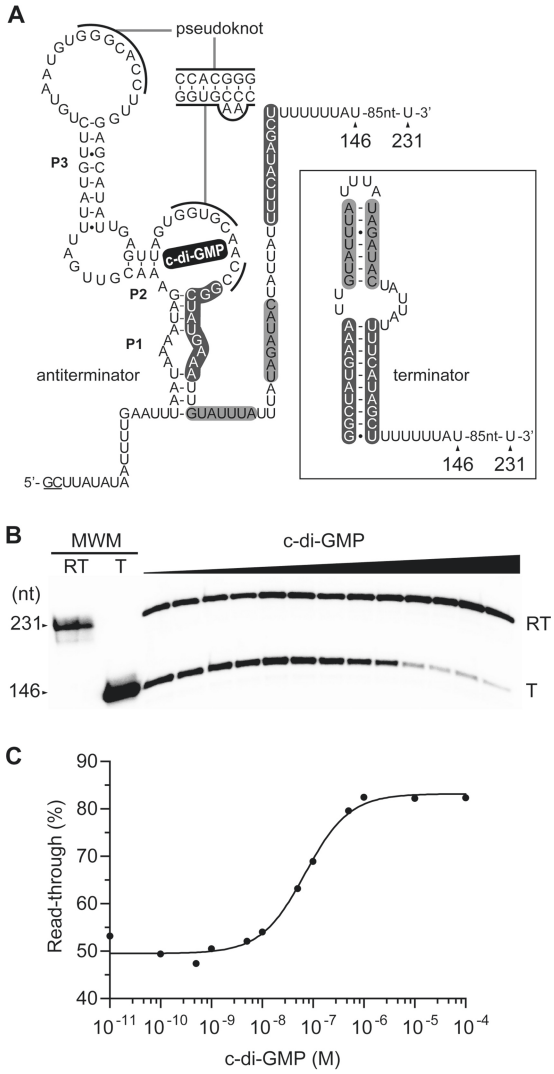

FIG 6 Cdi2_4 is a transcriptional c-di-GMP-II riboswitch. (A) Predicted Cdi2_4 c-di-GMP-II riboswitch-mediated transcription regulation. c-di-GMP is predicted to increase transcription past a predicted Rho-independent transcription terminator. Upon c-di-GMP binding to the aptamer, the P1 stem folds and sequesters nucleotides needed for the terminator formation and therefore acts as an antiterminator. Positions 231 and 146 correspond to the last nucleotides of the full-length transcript and the predicted terminated transcript, respectively. GC nucleotides (underlined) were added to the template for transcription priming using GC dinucleotides. The predicted Cdi2_4 aptamer is illustrated based on its predicted secondary structure (25). The transcription terminator folding was predicted using the RNAfold web server (http://rna.tbi.univie.ac.at/cgi-bin/RNAfold.cgi) (62). (B) Single-round *in vitro* transcription of the Cdi2_4 riboswitch template. Transcription reactions were carried out as a function of c-di-GMP concentration. Read-through (RT) and terminated (T) products are indicated on the right. Transcripts of 231 nt (RT) and 146 nt (T) were labeled and used as molecular size makers (MWM). The reactions were done in duplicate, and a representative image is shown. (C) The percentages of read-through products are plotted as a function of c-di-GMP concentration as quantified from panel B. The plot shows a two-state model from which a T_{50} value of 70 ± 12 nM c-di-GMP was calculated.

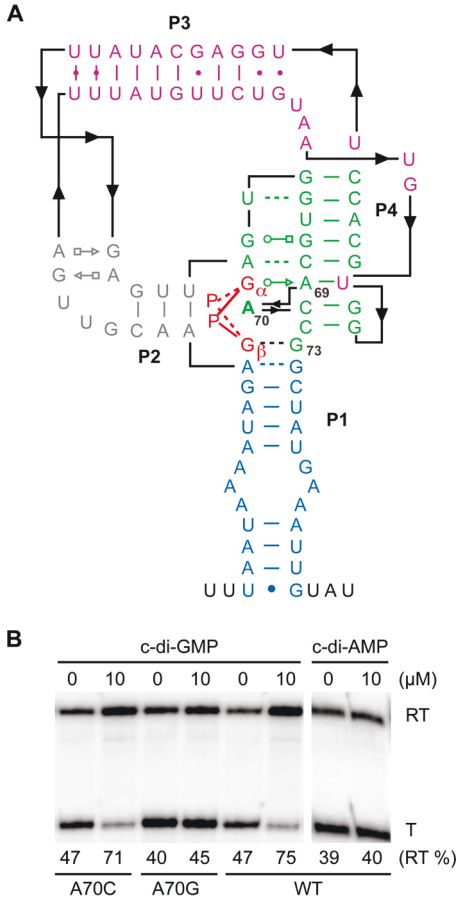

FIG 7 Cdi2_4 riboswitch transcription regulation requires specific c-di-GMP binding. (A) Predicted secondary structure and tertiary interactions of the Cdi2_4 aptamer upstream of *pilA1*. The cdi2_4 aptamer structure is based on the three-dimensional structure of the Cac-1-2 c-di-GMP-II aptamer from *Clostridium acetobutylicum* (64). For clarity, P1 (blue), P2 (gray), P3 (purple), and P4/pseudoknot (green) are shown in color. The c-di-GMP molecule is shown in red. Positions 69, 70, and 73 correspond to nucleotides interacting with c-di-GMP in Cac-1-2. Bases pairs are indicated with standard symbols (89). (B) Single-round *in vitro* transcription of the Cdi2-4 riboswitch. Transcription reactions were performed on DNA templates carrying no mutation (WT) or a single-nucleotide substitution (A70C and A70G) without or with 10 μM c-di-GMP or c-di-AMP. Read-through (RT) and terminated (T) products are indicated on the right. The percentages of read-through (RT %) products are indicated under every lane.

tinue to increase past about 0.3 while the *pilA1* mutant with pDccA-*RB*^{A70G}-*pilA1* reached and remained at an OD_{600} of ~0.5 as the cell aggregates accumulated at the bottoms of the tubes (Fig. 4B and C).

DISCUSSION

Insightful studies have revealed the versatility of functions conferred by T4P as well as the complexity of their assembly and regulation in Gram-negative bacteria. Recently, T4P were predicted to be also encoded by many Gram-positive bacteria (38–40). Yet, the role of T4P in Gram-positive bacteria has only been determined for the cellulolytic bacterium *Ruminococcus albus*, for which T4P are important for adhesion to cellulose (65), and *Clostridium perfringens*, for which T4P pilins appear at the bacterial surface and T4P are involved in gliding motility and biofilm formation (39, 66).

In this work, we have unraveled the contribution of T4P in the aggregation of *C. difficile* and the regulation of their synthesis by a c-di-GMP-dependent transcriptional riboswitch activator. Although our study represents the first genetic and functional char-

acterization of T4P in *C. difficile*, these structures were most likely observed much earlier. Borriello et al. (67) reported filaments measuring 4 to 9 nm in diameter and up to 6 μm long located at the poles of agar-grown cells, mostly gathered in bundles, although only 0 to 6% of the cells presented pilus-like structures depending on the strains. This is similar to the size of the T4P on the liquid-grown planktonic cells reported herein, which we only observed as single filaments. And while most cells displayed T4P at their surface, we also observed a noticeable population of cells devoid of T4P with high c-di-GMP levels. Although this observation could simply result from pilus breakages during sample preparation, we cannot rule out that T4P synthesis is subject to additional stochastic regulation mechanisms.

Recently Piepenbrink et al. (68) reported the display of T4P at the surface of *C. difficile* R20291 after anaerobic growth at 37°C on Columbia agar plates and prolonged incubation at room temperature. Composition analysis of these appendages by double immunogold staining revealed the presence of both PilA1 and PilJ in *C. difficile* R20291 pili (68). Despite that PilA1 is hypothesized to be the major pilin, the individual role of PilJ and PilA1 in the biogenesis of T4P in *C. difficile* 630 remains unknown. Yet, we clearly show that disruption of *pilA1* (or *pilB1*) abolished pilus formation and significantly reduced cell aggregation. Incidentally, the low residual pilus formation observed in the *pilB1* mutant background could result from a partial complementation by the second PilB protein, encoded by the *pilB2* gene. Ectopic expression of *pilA1* complemented the *pilA1* mutant of *C. difficile* 630 in cell aggregation experiments, confirming that PilA1 is a key factor for both T4P biogenesis and aggregation. We speculate that if PilJ or another pilin is the main component of *C. difficile* T4P, PilA1 might play a key regulatory role in the assembly of the pilus structure, as demonstrated for some minor pilins in other species (69–71). Therefore, the PilA1 pilin may indirectly contribute to T4P-mediated aggregation. Additional studies are required to understand the relative contribution of PilJ and PilA1 to T4P formation in *C. difficile* as well as the possible contribution of the three other predicted pilins encoded by the primary T4P locus, PilK, PilU, and PilV, and the two predicted pilins PilW and PilA2.

T4P were previously shown to be regulated by c-di-GMP in other bacteria. Most interestingly, the c-di-GMP-binding PilZ domain retains its name from the PilZ protein from *P. aeruginosa*, which is required for twitching motility and T4P biogenesis in this species (22, 72). Ironically, PilZ is the only one of the eight proteins containing a PilZ domain in *P. aeruginosa* that was unable to bind c-di-GMP in *in vitro* assays (73). However, the c-di-GMP-binding protein FimX is required for T4P biogenesis and twitching motility in *P. aeruginosa* (74–76). In *Xanthomonas axonopodis* pv. *citri*, the orthologous PilZ protein was shown to bind to both FimX and the ATPase PilB required for pilin polymerization (77). In these species, current evidence suggests that c-di-GMP regulates T4P biogenesis and function by mechanisms relying on protein-protein interactions. Riboswitch-mediated transcription regulation reported herein is a novel mechanism of T4P biogenesis regulation by c-di-GMP signaling.

While elevating intracellular c-di-GMP in *C. difficile* increased *pilA1* transcript levels by 30 to 40-fold, c-di-GMP increased Cdi2_4 riboswitch read-through transcription from 50% to 80% *in vitro*. Yet, it is not uncommon to observe a relatively modest change in transcription in single-round *in vitro* transcription assays compared to the observed cellular transcript levels (78–81). As for other *in vitro* assays, single-round transcription assays provide clear evidence of a biological process, although the results obtained may suffer from the inherent lack of complexity and/or from inaccuracy compared to biological systems. Nonetheless, the hypothesized transcriptional termination switch of riboswitch Cdi2_4 confirmed *in vitro* echoes recent unexplained results. Recently, Soutourina et al. (32) have identified regulatory RNAs in the whole genome of *C. difficile* 630 and confirmed the expression of the 12 c-di-GMP-I and 4 c-di-GMP-II predicted riboswitches. The authors reported increased *pilA1* (CD3513) transcript levels and observed only full-length transcripts upon increasing c-di-GMP levels. They reasonably hypothesized that the full-length transcripts were stabilized only under the condition of elevated c-di-GMP because of active translation of PilA1, assuming that all 4 c-di-GMP-II riboswitches have the same expression platform as Cdi2_1, which contains an ~600-nt self-splicing group I intron promoting translation of the CD3246 putative surface protein upon binding of c-di-GMP to the aptamer (25, 82). However, this self-splicing group I ribozyme is the only one among the 10 representative ribozymes predicted in strain 630 to be located near a c-di-GMP riboswitch (25). Although translation of the full-length transcripts upon increasing c-di-GMP levels may still contribute to *pilA1* transcript stability, our results suggest that c-di-GMP increases *pilA1* transcript levels through binding to a transcriptionally activating c-di-GMP riboswitch rather than by promoting *pilA1* translation.

The exact mechanism leading to T4P-dependent cell aggregation and its role in the physiology and pathogenesis of *C. difficile* remain to be determined. It is reasonable to presume that T4P may also be involved in other phenotypes in *C. difficile*, such as biofilm formation, which was recently reported to be induced by c-di-GMP (32). *C. difficile* cells can grow *in vitro* on abiotic surfaces embedded within a biofilm matrix containing exopolysaccharides, DNA, and proteins, which increases resistance of vegetative cells to oxidative stress and vancomycin (83, 84). Hypothetically, autoaggregation could promote biofilm formation in its early stages. However, preliminary experiments did not show a clear contribution of T4P or c-di-GMP to biofilm formation, as the phenotype was weak and variable under our experimental conditions. Biofilm formation in *C. difficile* was reported to be weaker with strain 630 than with strain R20291 (84), and perhaps the latter, and other strains, should be used in future studies to ascertain the role of T4P in *C. difficile*.

Nevertheless, we speculate that T4P are involved in the pathogenicity of *C. difficile*. Multicellular structures of *C. difficile* cells, described as cell aggregates, were observed in a mouse model of colonization and suggest that aggregation and/or biofilm could be important for colonization (85). Goulding et al. (86) also detected the presence of pilus-like structures at the surface of *C. difficile* cells within the intestinal crypts of infected hamsters and detected the predicted pilin CD3507 *in vivo*. These observations and our results confirmed that T4P are produced at the cell surface and suggest that these appendages are important for host colonization and pathogenesis of *C. difficile*.

ACKNOWLEDGMENTS

We thank Robert McKee, Adam Spaulding, and Ankunda Kariisa for their assistance in enumerating pili for the electron microscopy studies and Mihnea Mangalea for the construction of the *sigD* mutant.

This work was supported by a grant from the FRQNT Research Team

program to V.B. and L.-C.F., an Alexander Graham Bell Canada Graduate Scholarship from the NSERC to E.B., and NIH awards T32-DK007737 to E.B.P. and U54-AI057157 and R01-AI107029 to R.T. V.B. holds a Canada Research Chair in Bacterial Molecular Genetics.

The funders had no role in study design, data collection and analysis, decision to publish, or preparation of the manuscript.

REFERENCES

1. **Rupnik M, Wilcox MH, Gerding DN.** 2009. *Clostridium difficile* infection: new developments in epidemiology and pathogenesis. Nat Rev Microbiol **7:**526–536. http://dx.doi.org/10.1038/nrmicro2164.
2. **Giel JL, Sorg JA, Sonenshein AL, Zhu J.** 2010. Metabolism of bile salts in mice influences spore germination in *Clostridium difficile*. PLoS One **5:**e8740. http://dx.doi.org/10.1371/journal.pone.0008740.
3. **Wilson KH, Sheagren JN, Freter R.** 1985. Population dynamics of ingested *Clostridium difficile* in the gastrointestinal tract of the Syrian hamster. J Infect Dis **151:**355–361. http://dx.doi.org/10.1093/infdis/151.2.355.
4. **Dineen SS, Villapakkam AC, Nordman JT, Sonenshein AL.** 2007. Repression of *Clostridium difficile* toxin gene expression by CodY. Mol Microbiol **66:**206–219. http://dx.doi.org/10.1111/j.1365-2958.2007.05906.x.
5. **El Meouche I, Peltier J, Monot M, Soutourina O, Pestel-Caron M, Dupuy B, Pons JL.** 2013. Characterization of the SigD regulon of *C. difficile* and its positive control of toxin production through the regulation of tcdR. PLoS One **8:**e83748. http://dx.doi.org/10.1371/journal.pone.0083748.
6. **Ho TD, Ellermeier CD.** 2011. PrsW is required for colonization, resistance to antimicrobial peptides, and expression of extracytoplasmic function sigma factors in *Clostridium difficile*. Infect Immun **79:**3229–3238. http://dx.doi.org/10.1128/IAI.00019-11.
7. **Mani N, Dupuy B.** 2001. Regulation of toxin synthesis in *Clostridium difficile* by an alternative RNA polymerase sigma factor. Proc Natl Acad Sci U S A **98:**5844–5849. http://dx.doi.org/10.1073/pnas.101126598.
8. **Martin MJ, Clare S, Goulding D, Faulds-Pain A, Barquist L, Browne HP, Pettit L, Dougan G, Lawley TD, Wren BW.** 2013. The *agr* locus regulates virulence and colonization genes in *Clostridium difficile* 027. J Bacteriol **195:**3672–3681. http://dx.doi.org/10.1128/JB.00473-13.
9. **Saujet L, Monot M, Dupuy B, Soutourina O, Martin-Verstraete I.** 2011. The key sigma factor of transition phase, SigH, controls sporulation, metabolism, and virulence factor expression in *Clostridium difficile*. J Bacteriol **193:**3186–3196. http://dx.doi.org/10.1128/JB.00272-11.
10. **Hengge R.** 2009. Principles of c-di-GMP signalling in bacteria. Nat Rev Microbiol **7:**263–273. http://dx.doi.org/10.1038/nrmicro2109.
11. **Römling U, Galperin MY, Gomelsky M.** 2013. Cyclic di-GMP: the first 25 years of a universal bacterial second messenger. Microbiol Mol Biol Rev **77:**1–52. http://dx.doi.org/10.1128/MMBR.00043-12.
12. **Tamayo R, Pratt JT, Camilli A.** 2007. Roles of cyclic diguanylate in the regulation of bacterial pathogenesis. Annu Rev Microbiol **61:**131–148. http://dx.doi.org/10.1146/annurev.micro.61.080706.093426.
13. **Aldridge P, Paul R, Goymer P, Rainey P, Jenal U.** 2003. Role of the GGDEF regulator PleD in polar development of *Caulobacter crescentus*. Mol Microbiol **47:**1695–1708. http://dx.doi.org/10.1046/j.1365-2958.2003.03401.x.
14. **Tischler AD, Camilli A.** 2005. Cyclic diguanylate regulates *Vibrio cholerae* virulence gene expression. Infect Immun **73:**5873–5882. http://dx.doi.org/10.1128/IAI.73.9.5873-5882.2005.
15. **Pitzer JE, Sultan SZ, Hayakawa Y, Hobbs G, Miller MR, Motaleb MA.** 2011. Analysis of the *Borrelia burgdorferi* cyclic-di-GMP-binding protein PlzA reveals a role in motility and virulence. Infect Immun **79:**1815–1825. http://dx.doi.org/10.1128/IAI.00075-11.
16. **Kulasakara H, Lee V, Brencic A, Liberati N, Urbach J, Miyata S, Lee DG, Neely AN, Hyodo M, Hayakawa Y, Ausubel FM, Lory S.** 2006. Analysis of *Pseudomonas aeruginosa* diguanylate cyclases and phosphodiesterases reveals a role for bis-(3′-5′)-cyclic-GMP in virulence. Proc Natl Acad Sci U S A **103:**2839–2844. http://dx.doi.org/10.1073/pnas.0511090103.
17. **Ryan RP, Fouhy Y, Lucey JF, Crossman LC, Spiro S, He YW, Zhang LH, Heeb S, Camara M, Williams P, Dow JM.** 2006. Cell-cell signaling in *Xanthomonas campestris* involves an HD-GYP domain protein that functions in cyclic di-GMP turnover. Proc Natl Acad Sci U S A **103:**6712–6717. http://dx.doi.org/10.1073/pnas.0600345103.
18. **Ryjenkov DA, Tarutina M, Moskvin OV, Gomelsky M.** 2005. Cyclic diguanylate is a ubiquitous signaling molecule in bacteria: insights into biochemistry of the GGDEF protein domain. J Bacteriol **187:**1792–1798. http://dx.doi.org/10.1128/JB.187.5.1792-1798.2005.
19. **Schmidt AJ, Ryjenkov DA, Gomelsky M.** 2005. The ubiquitous protein domain EAL is a cyclic diguanylate-specific phosphodiesterase: enzymatically active and inactive EAL domains. J Bacteriol **187:**4774–4781. http://dx.doi.org/10.1128/JB.187.14.4774-4781.2005.
20. **Simm R, Morr M, Kader A, Nimtz M, Romling U.** 2004. GGDEF and EAL domains inversely regulate cyclic di-GMP levels and transition from sessility to motility. Mol Microbiol **53:**1123–1134. http://dx.doi.org/10.1111/j.1365-2958.2004.04206.x.
21. **Tamayo R, Tischler AD, Camilli A.** 2005. The EAL domain protein VieA is a cyclic diguanylate phosphodiesterase. J Biol Chem **280:**33324–33330. http://dx.doi.org/10.1074/jbc.M506500200.
22. **Amikam D, Galperin MY.** 2006. PilZ domain is part of the bacterial c-di-GMP binding protein. Bioinformatics **22:**3–6. http://dx.doi.org/10.1093/bioinformatics/bti739.
23. **Hickman JW, Harwood CS.** 2008. Identification of FleQ from *Pseudomonas aeruginosa* as a c-di-GMP-responsive transcription factor. Mol Microbiol **69:**376–389. http://dx.doi.org/10.1111/j.1365-2958.2008.06281.x.
24. **Krasteva PV, Fong JC, Shikuma NJ, Beyhan S, Navarro MV, Yildiz FH, Sondermann H.** 2010. *Vibrio cholerae* VpsT regulates matrix production and motility by directly sensing cyclic di-GMP. Science **327:**866–868. http://dx.doi.org/10.1126/science.1181185.
25. **Lee ER, Baker JL, Weinberg Z, Sudarsan N, Breaker RR.** 2010. An allosteric self-splicing ribozyme triggered by a bacterial second messenger. Science **329:**845–848. http://dx.doi.org/10.1126/science.1190713.
26. **Sudarsan N, Lee ER, Weinberg Z, Moy RH, Kim JN, Link KH, Breaker RR.** 2008. Riboswitches in eubacteria sense the second messenger cyclic di-GMP. Science **321:**411–413. http://dx.doi.org/10.1126/science.1159519.
27. **Breaker RR.** 2012. Riboswitches and the RNA world. Cold Spring Harb Perspect Biol **4**(2):a003566. http://dx.doi.org/10.1101/cshperspect.a003566.
28. **Serganov A, Nudler E.** 2013. A decade of riboswitches. Cell **152:**17–24. http://dx.doi.org/10.1016/j.cell.2012.12.024.
29. **Bordeleau E, Fortier LC, Malouin F, Burrus V.** 2011. c-di-GMP turnover in *Clostridium difficile* is controlled by a plethora of diguanylate cyclases and phosphodiesterases. PLoS Genet **7:**e1002039. http://dx.doi.org/10.1371/journal.pgen.1002039.
30. **Gao X, Dong X, Subramanian S, Matthews PM, Cooper CA, Kearns DB, Dann CE, III.** 2014. Engineered *Bacillus subtilis* strains allow for rapid characterization of heterologous diguanylate cyclases and phosphodiesterases. Appl Environ Microbiol **80:**6167–6174. http://dx.doi.org/10.1128/AEM.01638-14.
31. **Purcell EB, McKee RW, McBride SM, Waters CM, Tamayo R.** 2012. Cyclic diguanylate inversely regulates motility and aggregation in *Clostridium difficile*. J Bacteriol **194:**3307–3316. http://dx.doi.org/10.1128/JB.00100-12.
32. **Soutourina OA, Monot M, Boudry P, Saujet L, Pichon C, Sismeiro O, Semenova E, Severinov K, Le Bouguenec C, Coppee JY, Dupuy B, Martin-Verstraete I.** 2013. Genome-wide identification of regulatory RNAs in the human pathogen *Clostridium difficile*. PLoS Genet **9:**e1003493. http://dx.doi.org/10.1371/journal.pgen.1003493.
33. **Cafardi V, Biagini M, Martinelli M, Leuzzi R, Rubino JT, Cantini F, Norais N, Scarselli M, Serruto D, Unnikrishnan M.** 2013. Identification of a novel zinc metalloprotease through a global analysis of *Clostridium difficile* extracellular proteins. PLoS One **8:**e81306. http://dx.doi.org/10.1371/journal.pone.0081306.
34. **Hensbergen PJ, Klychnikov OI, Bakker D, van Winden VJ, Ras N, Kemp AC, Cordfunke RA, Dragan I, Deelder AM, Kuijper EJ, Corver J, Drijfhout JW, van Leeuwen HC.** 2014. A novel secreted metalloprotease (CD2830) from *Clostridium difficile* cleaves specific proline sequences in LPXTG cell surface proteins. Mol Cell Proteomics **13:**1231–1244. http://dx.doi.org/10.1074/mcp.M113.034728.
35. **Giltner CL, Nguyen Y, Burrows LL.** 2012. Type IV pilin proteins: versatile molecular modules. Microbiol Mol Biol Rev **76:**740–772. http://dx.doi.org/10.1128/MMBR.00035-12.
36. **Proft T, Baker EN.** 2009. Pili in Gram-negative and Gram-positive bacteria—structure, assembly and their role in disease. Cell Mol Life Sci **66:**613–635. http://dx.doi.org/10.1007/s00018-008-8477-4.
37. **Craig L, Li J.** 2008. Type IV pili: paradoxes in form and function. Curr Opin Struct Biol **18:**267–277. http://dx.doi.org/10.1016/j.sbi.2007.12.009.

38. **Sebaihia M, Wren BW, Mullany P, Fairweather NF, Minton N, Stabler R, Thomson NR, Roberts AP, Cerdeno-Tarraga AM, Wang H, Holden MT, Wright A, Churcher C, Quail MA, Baker S, Bason N, Brooks K, Chillingworth T, Cronin A, Davis P, Dowd L, Fraser A, Feltwell T, Hance Z, Holroyd S, Jagels K, Moule S, Mungall K, Price C, Rabbinowitsch E, Sharp S, Simmonds M, Stevens K, Unwin L, Whithead S, Dupuy B, Dougan G, Barrell B, Parkhill J.** 2006. The multidrug-resistant human pathogen *Clostridium difficile* has a highly mobile, mosaic genome. Nat Genet **38:**779–786. http://dx.doi.org/10.1038/ng1830.
39. **Varga JJ, Nguyen V, O'Brien DK, Rodgers K, Walker RA, Melville SB.** 2006. Type IV pili-dependent gliding motility in the Gram-positive pathogen *Clostridium perfringens* and other Clostridia. Mol Microbiol **62:**680–694. http://dx.doi.org/10.1111/j.1365-2958.2006.05414.x.
40. **Imam S, Chen Z, Roos DS, Pohlschroder M.** 2011. Identification of surprisingly diverse type IV pili, across a broad range of Gram-positive bacteria. PLoS One **6:**e28919. http://dx.doi.org/10.1371/journal.pone.0028919.
41. **Melville S, Craig L.** 2013. Type IV pili in Gram-positive bacteria. Microbiol Mol Biol Rev **77:**323–341. http://dx.doi.org/10.1128/MMBR.00063-12.
42. **Maldarelli GA, De Masi L, von Rosenvinge EC, Carter M, Donnenberg MS.** 2014. Identification, immunogenicity, and cross-reactivity of type IV pilin and pilin-like proteins from *Clostridium difficile*. Pathog Dis **71:**302–314. http://dx.doi.org/10.1111/2049-632X.12137.
43. **Smith CJ, Markowitz SM, Macrina FL.** 1981. Transferable tetracycline resistance in *Clostridium difficile*. Antimicrob Agents Chemother **19:**997–1003. http://dx.doi.org/10.1128/AAC.19.6.997.
44. **Karberg M, Guo H, Zhong J, Coon R, Perutka J, Lambowitz AM.** 2001. Group II introns as controllable gene targeting vectors for genetic manipulation of bacteria. Nat Biotechnol **19:**1162–1167. http://dx.doi.org/10.1038/nbt1201-1162.
45. **Heap JT, Kuehne SA, Ehsaan M, Cartman ST, Cooksley CM, Scott JC, Minton NP.** 2010. The ClosTron: mutagenesis in *Clostridium* refined and streamlined. J Microbiol Methods **80:**49–55. http://dx.doi.org/10.1016/j.mimet.2009.10.018.
46. **Perutka J, Wang W, Goerlitz D, Lambowitz AM.** 2004. Use of computer-designed group II introns to disrupt *Escherichia coli* DExH/D-box protein and DNA helicase genes. J Mol Biol **336:**421–439. http://dx.doi.org/10.1016/j.jmb.2003.12.009.
47. **Heap JT, Cartman ST, Kuehne SA, Cooksley C, Minton NP.** 2010. ClosTron-targeted mutagenesis. Methods Mol Biol **646:**165–182. http://dx.doi.org/10.1007/978-1-60327-365-7_11.
48. **Bouillaut L, Self WT, Sonenshein AL.** 2013. Proline-dependent regulation of *Clostridium difficile* Stickland metabolism. J Bacteriol **195:**844–854. http://dx.doi.org/10.1128/JB.01492-12.
49. **Stemmer WP, Crameri A, Ha KD, Brennan TM, Heyneker HL.** 1995. Single-step assembly of a gene and entire plasmid from large numbers of oligodeoxyribonucleotides. Gene **164:**49–53. http://dx.doi.org/10.1016/0378-1119(95)00511-4.
50. **Colmin C, Pebay M, Simonet JM, Decaris B.** 1991. A species-specific DNA probe obtained from *Streptococcus salivarius* subsp. *thermophilus* detects strain restriction polymorphism FEMS Microbiol Lett **65:**123–128.
51. **Dower WJ, Miller JF, Ragsdale CW.** 1988. High efficiency transformation of *E. coli* by high voltage electroporation. Nucleic Acids Res **16:**6127–6145. http://dx.doi.org/10.1093/nar/16.13.6127.
52. **Hellemans J, Mortier G, De Paepe A, Speleman F, Vandesompele J.** 2007. qBase relative quantification framework and software for management and automated analysis of real-time quantitative PCR data. Genome Biol **8:**R19. http://dx.doi.org/10.1186/gb-2007-8-2-r19.
53. **Vandesompele J, De Preter K, Pattyn F, Poppe B, Van Roy N, De Paepe A, Speleman F.** 2002. Accurate normalization of real-time quantitative RT-PCR data by geometric averaging of multiple internal control genes. Genome Biol **3:**RESEARCH0034. http://dx.doi.org/10.1186/gb-2002-3-7-research0034.
54. **Brosseau JP, Lucier JF, Lapointe E, Durand M, Gendron D, Gervais-Bird J, Tremblay K, Perreault JP, Elela SA.** 2010. High-throughput quantification of splicing isoforms. RNA **16:**442–449. http://dx.doi.org/10.1261/rna.1877010.
55. **Blouin S, Lafontaine DA.** 2007. A loop loop interaction and a K-turn motif located in the lysine aptamer domain are important for the riboswitch gene regulation control. RNA **13:**1256–1267. http://dx.doi.org/10.1261/rna.560307.
56. **Pleiss JA, Derrick ML, Uhlenbeck OC.** 1998. T7 RNA polymerase produces 5′ end heterogeneity during in vitro transcription from certain templates. RNA **4:**1313–1317. http://dx.doi.org/10.1017/S135583829800106X.
57. **Freitag NE, Seifert HS, Koomey M.** 1995. Characterization of the *pilF-pilD* pilus-assembly locus of *Neisseria gonorrhoeae*. Mol Microbiol **16:**575–586. http://dx.doi.org/10.1111/j.1365-2958.1995.tb02420.x.
58. **Turner LR, Lara JC, Nunn DN, Lory S.** 1993. Mutations in the consensus ATP-binding sites of XcpR and PilB eliminate extracellular protein secretion and pilus biogenesis in *Pseudomonas aeruginosa*. J Bacteriol **175:**4962–4969.
59. **Aubry A, Hussack G, Chen W, KuoLee R, Twine SM, Fulton KM, Foote S, Carrillo CD, Tanha J, Logan SM.** 2012. Modulation of toxin production by the flagellar regulon in *Clostridium difficile*. Infect Immun **80:**3521–3532. http://dx.doi.org/10.1128/IAI.00224-12.
60. **Strom MS, Lory S.** 1991. Amino acid substitutions in pilin of *Pseudomonas aeruginosa*. Effect on leader peptide cleavage, amino-terminal methylation, and pilus assembly. J Biol Chem **266:**1656–1664.
61. **Mitra A, Kesarwani AK, Pal D, Nagaraja V.** 2011. WebGeSTer DB—a transcription terminator database. Nucleic Acids Res **39:**D129–D135. http://dx.doi.org/10.1093/nar/gkq971.
62. **Gruber AR, Lorenz R, Bernhart SH, Neubock R, Hofacker IL.** 2008. The Vienna RNA websuite. Nucleic Acids Res **36:**W70–W74. http://dx.doi.org/10.1093/nar/gkn188.
63. **Wickiser JK, Winkler WC, Breaker RR, Crothers DM.** 2005. The speed of RNA transcription and metabolite binding kinetics operate an FMN riboswitch. Mol Cell **18:**49–60. http://dx.doi.org/10.1016/j.molcel.2005.02.032.
64. **Smith KD, Shanahan CA, Moore EL, Simon AC, Strobel SA.** 2011. Structural basis of differential ligand recognition by two classes of bis-(3′-5′)-cyclic dimeric guanosine monophosphate-binding riboswitches. Proc Natl Acad Sci U S A **108:**7757–7762. http://dx.doi.org/10.1073/pnas.1018857108.
65. **Rakotoarivonina H, Jubelin G, Hebraud M, Gaillard-Martinie B, Forano E, Mosoni P.** 2002. Adhesion to cellulose of the Gram-positive bacterium *Ruminococcus albus* involves type IV pili. Microbiology **148:**1871–1880.
66. **Varga JJ, Therit B, Melville SB.** 2008. Type IV pili and the CcpA protein are needed for maximal biofilm formation by the Gram-positive anaerobic pathogen *Clostridium perfringens*. Infect Immun **76:**4944–4951. http://dx.doi.org/10.1128/IAI.00692-08.
67. **Borriello SP, Davies HA, Barclay FE.** 1988. Detection of fimbriae amongst strains of *Clostridium difficile*. FEMS Microbiol Lett **49:**65–67. http://dx.doi.org/10.1111/j.1574-6968.1988.tb02683.x.
68. **Piepenbrink KH, Maldarelli GA, de la Pena CF, Mulvey GL, Snyder GA, De Masi L, von Rosenvinge EC, Gunther S, Armstrong GD, Donnenberg MS, Sundberg EJ.** 2014. Structure of *Clostridium difficile* PilJ exhibits unprecedented divergence from known type IV pilins. J Biol Chem **289:**4334–4345. http://dx.doi.org/10.1074/jbc.M113.534404.
69. **Giltner CL, Habash M, Burrows LL.** 2010. *Pseudomonas aeruginosa* minor pilins are incorporated into type IV pili. J Mol Biol **398:**444–461. http://dx.doi.org/10.1016/j.jmb.2010.03.028.
70. **Nair DB, Chung DK, Schneider J, Uchida K, Aizawa S, Jarrell KF.** 2013. Identification of an additional minor pilin essential for piliation in the archaeon *Methanococcus maripaludis*. PLoS One **8:**e83961. http://dx.doi.org/10.1371/journal.pone.0083961.
71. **Winther-Larsen HC, Wolfgang M, Dunham S, van Putten JP, Dorward D, Lovold C, Aas FE, Koomey M.** 2005. A conserved set of pilin-like molecules controls type IV pilus dynamics and organelle-associated functions in *Neisseria gonorrhoeae*. Mol Microbiol **56:**903–917. http://dx.doi.org/10.1111/j.1365-2958.2005.04591.x.
72. **Alm RA, Bodero AJ, Free PD, Mattick JS.** 1996. Identification of a novel gene, *pilZ*, essential for type 4 fimbrial biogenesis in *Pseudomonas aeruginosa*. J Bacteriol **178:**46–53.
73. **Merighi M, Lee VT, Hyodo M, Hayakawa Y, Lory S.** 2007. The second messenger bis-(3′-5′)-cyclic-GMP and its PilZ domain-containing receptor Alg44 are required for alginate biosynthesis in *Pseudomonas aeruginosa*. Mol Microbiol **65:**876–895. http://dx.doi.org/10.1111/j.1365-2958.2007.05817.x.
74. **Huang B, Whitchurch CB, Mattick JS.** 2003. FimX, a multidomain protein connecting environmental signals to twitching motility in *Pseudomonas aeruginosa*. J Bacteriol **185:**7068–7076. http://dx.doi.org/10.1128/JB.185.24.7068-7076.2003.
75. **Jain R, Behrens AJ, Kaever V, Kazmierczak BI.** 2012. Type IV pilus assembly in *Pseudomonas aeruginosa* over a broad range of cyclic di-GMP

concentrations. J Bacteriol **194:**4285–4294. http://dx.doi.org/10.1128/JB.00803-12.

76. **Kazmierczak BI, Lebron MB, Murray TS.** 2006. Analysis of FimX, a phosphodiesterase that governs twitching motility in *Pseudomonas aeruginosa*. Mol Microbiol **60:**1026–1043. http://dx.doi.org/10.1111/j.1365-2958.2006.05156.x.
77. **Guzzo CR, Salinas RK, Andrade MO, Farah CS.** 2009. PILZ protein structure and interactions with PILB and the FIMX EAL domain: implications for control of type IV pilus biogenesis. J Mol Biol **393:**848–866. http://dx.doi.org/10.1016/j.jmb.2009.07.065.
78. **Lemay JF, Penedo JC, Tremblay R, Lilley DM, Lafontaine DA.** 2006. Folding of the adenine riboswitch. Chem Biol **13:**857–868. http://dx.doi.org/10.1016/j.chembiol.2006.06.010.
79. **Lemay JF, Desnoyers G, Blouin S, Heppell B, Bastet L, St-Pierre P, Masse E, Lafontaine DA.** 2011. Comparative study between transcriptionally- and translationally-acting adenine riboswitches reveals key differences in riboswitch regulatory mechanisms. PLoS Genet **7:**e1001278. http://dx.doi.org/10.1371/journal.pgen.1001278.
80. **Heppell B, Blouin S, Dussault AM, Mulhbacher J, Ennifar E, Penedo JC, Lafontaine DA.** 2011. Molecular insights into the ligand-controlled organization of the SAM-I riboswitch. Nat Chem Biol **7:**384–392. http://dx.doi.org/10.1038/nchembio.563.
81. **Winkler WC, Nahvi A, Sudarsan N, Barrick JE, Breaker RR.** 2003. An mRNA structure that controls gene expression by binding S-adenosylmethionine. Nat Struct Biol **10:**701–707. http://dx.doi.org/10.1038/nsb967.
82. **Chen AG, Sudarsan N, Breaker RR.** 2011. Mechanism for gene control by a natural allosteric group I ribozyme. RNA **17:**1967–1972. http://dx.doi.org/10.1261/rna.2757311.
83. **Dawson LF, Valiente E, Faulds-Pain A, Donahue EH, Wren BW.** 2012. Characterisation of *Clostridium difficile* biofilm formation, a role for Spo0A. PLoS One **7:**e50527. http://dx.doi.org/10.1371/journal.pone.0050527.
84. **Dapa T, Leuzzi R, Ng YK, Baban ST, Adamo R, Kuehne SA, Scarselli M, Minton NP, Serruto D, Unnikrishnan M.** 2013. Multiple factors modulate biofilm formation by the anaerobic pathogen *Clostridium difficile*. J Bacteriol **195:**545–555. http://dx.doi.org/10.1128/JB.01980-12.
85. **Lawley TD, Clare S, Walker AW, Goulding D, Stabler RA, Croucher N, Mastroeni P, Scott P, Raisen C, Mottram L, Fairweather NF, Wren BW, Parkhill J, Dougan G.** 2009. Antibiotic treatment of *Clostridium difficile* carrier mice triggers a supershedder state, spore-mediated transmission, and severe disease in immunocompromised hosts. Infect Immun **77:**3661–3669. http://dx.doi.org/10.1128/IAI.00558-09.
86. **Goulding D, Thompson H, Emerson J, Fairweather NF, Dougan G, Douce GR.** 2009. Distinctive profiles of infection and pathology in hamsters infected with *Clostridium difficile* strains 630 and B1. Infect Immun **77:**5478–5485. http://dx.doi.org/10.1128/IAI.00551-09.
87. **Hussain HA, Roberts AP, Mullany P.** 2005. Generation of an erythromycin-sensitive derivative of *Clostridium difficile* strain 630 (630Δ*erm*) and demonstration that the conjugative transposon Tn*916*ΔE enters the genome of this strain at multiple sites. J Med Microbiol **54:**137–141. http://dx.doi.org/10.1099/jmm.0.45790-0.
88. **Purdy D, O'Keeffe TA, Elmore M, Herbert M, McLeod A, Bokori-Brown M, Ostrowski A, Minton NP.** 2002. Conjugative transfer of clostridial shuttle vectors from *Escherichia coli* to *Clostridium difficile* through circumvention of the restriction barrier. Mol Microbiol **46:**439–452. http://dx.doi.org/10.1046/j.1365-2958.2002.03134.x.
89. **Leontis NB, Westhof E.** 2001. Geometric nomenclature and classification of RNA base pairs. RNA **7:**499–512. http://dx.doi.org/10.1017/S1355838201002515.